Received: 17 April 2019 | Revised: 18 June 2019 | Accepted: 11 July 2019

DOI: 10.1111/pce.13613

ORIGINAL ARTICLE

WILEY Plant, Cell & Environment

Morphological and physiological traits in relation to carbon balance in a diverse clade of dryland mosses

Kirsten K. Coe[1] | Nora B. Howard[1] | Mandy L. Slate[2] | Matthew A. Bowker[3] | Brent D. Mishler[4] | Riley Butler[2] | Joshua Greenwood[5] | Lloyd R. Stark[5]

[1] Department of Biology, St. Mary's College of Maryland, St. Mary'sCity, MD 20653, USA

[2] Division of Biological Sciences, University of Montana, Missoula, MT 59812, USA

[3] School of Forestry, Northern Arizona University, Flagstaff, AZ 86011, USA

[4] University and Jepson Herbaria, and Department of Integrative Biology, University of California Berkeley, Berkeley, CA 94720-2465, USA

[5] School of Life Sciences, University of Nevada Las Vegas, Las Vegas, NV 89154, USA

Correspondence
K. K. Coe, Department of Biology, Middlebury College, Middlebury, VT 05753, USA.
Email: kcoe@middlebury.edu

Funding information
Directorate for Biological Sciences, Grant/Award Numbers: 1638943, 1638955, 1638956 and 1638966; National Science Foundation Dimensions of Biodiversity Program Awards, Grant/Award Numbers: 1638943, 1638956, 1638966 and 1638955

Abstract

Plant functional trait analyses have focused almost exclusively on vascular plants, but bryophytes comprise ancient and diverse plant lineages that have widespread global distributions and important ecological functions in terrestrial ecosystems. We examined a diverse clade of dryland mosses, *Syntrichia*, and studied carbon balance during a precipitation event (C-balance), a functional trait related to physiological functioning, desiccation tolerance, survival, and ecosystem carbon and nitrogen cycling. We examined variability in C-balance among 14 genotypes of *Syntrichia* and measured an additional 10 physiological and 13 morphological traits at the cell, leaf, shoot, and clump level. C-balance varied 20-fold among genotypes, and highest C-balances were associated with long, narrow leaves with awns, and small cells with thick cell walls, traits that may influence water uptake and retention during a precipitation event. Ordination analyses revealed that the axis most strongly correlated with C-balance included the maximum chlorophyll fluorescence, F_m, indicating the importance of photosystem II health for C exchange. C-balance represents a key functional trait in bryophytes, but its measurement is time intensive and not feasible to measure on large scales. We propose two models (using physiological and morphological traits) to predict C-balance, whereby identifying simpler to measure traits for trait databases.

KEYWORDS

biocrust, bryophyte, desiccation tolerance, functional trait, photosynthesis, precipitation, water relations

1 | INTRODUCTION

In order to capture ecological dynamics across scales of organization, it is necessary to connect organismal form and function with physiological and ecosystem processes. Analyses are being developed to identify traits that are causally related to ecosystem processes and the occupation of specific environments. Such "functional traits" (Gitay & Noble, 1997; Lavorel, McIntyre, Landsberg, & Forbes, 1997) can then be used to predict plant responses to environmental change and forecast carbon (C), nitrogen (N), and hydrological cycling in terrestrial ecosystems (Anderegg, 2015; Cadotte, Cavender-Bares, Tilman, & Oakley, 2009; Cornwell et al., 2008; Craine et al., 2002; Díaz et al., 2016; Matheny, Mirfenderesgi, & Bohrer, 2017). Plant functional traits have been historically divided into *response traits*, adaptations allowing growth and reproduction in a given environment, and *effect traits*, those directly influencing community- and ecosystem-level processes (Lavorel & Garnier, 2002). Not surprisingly, response and effect traits have been shown to be inexorably linked in many ecosystems, where leaf and plant-level adaptations (e.g., growth rates, tissue C:N) can contribute to ecosystem level properties (e.g., net primary

productivity and decomposition rates; Cornelissen, Lang, Soudzilovskaia, & During, 2007; Suding et al., 2008). Furthermore, some functional traits (e.g., C exchange rates) may also fall into both categories simultaneously, representing important focal traits for modelling links between physiology and ecosystem processes at the community and ecosystem levels.

Analytical frameworks and associated databases for plant functional traits have to date focused on vascular plants (e.g., Anderegg, 2015; Cornelissen et al., 2003; Díaz et al., 2016; Weiner, Campbell, Pino, & Echarte, 2009; Wright et al., 2004). Bryophytes (mosses, liverworts, and hornworts), however, can contribute substantially to primary productivity, biogeochemistry, and ecology in many ecosystems (Lindo & Gonzalez, 2010; Street et al., 2013; Turetsky, 2003) and exhibit structural and physiological characteristics at the cell, shoot, and clump level that can be very distinct from vascular plants. This has led to recent efforts to develop predictive trait-based analytical frameworks for these groups of organisms (reviewed in Turetsky et al., 2012; Laing, Granath, Belyea, Allton, & Rydin, 2014; Mallen-Cooper & Eldridge, 2016; Deane-Coe & Stanton, 2017).

Trait-based studies on bryophytes have illustrated the diversity of morphological and physiological traits across species, clades (Kraichak, 2012; Waite & Sack, 2010; Wang, Bader, Liu, Zhu, & Bao, 2017; Wang, Bao, Feng, & Lin, 2014), sexes (Shaw & Gaughan, 1993; Slate, Rosenstiel, & Eppley, 2017), and within the diverse genus *Sphagnum* (Rice, Aclander, & Hanson, 2008). These studies have demonstrated how suites of physiological, morphological, and structural traits in bryophytes can be intercorrelated and also illustrate how variable some traits can be within and among species. Although functional trait-process patterns hold across many plant groups, tracheophytes and bryophytes can also differ in terms of relationships between functional traits and key ecological processes, one notable example being C uptake (Rice et al., 2008). In bryophytes, structural support traits (e.g., costa thickness, area, and length) often correlate with leaf size (Waite & Sack, 2010), illustrating the consistency of leaf level tradeoffs across plant groups. Also, certain physiological traits (i.e., light-saturated photosynthetic rate and chlorophyll content) are often correlated with light environment (Marschall & Proctor, 2004; Waite & Sack, 2010), but, unlike vascular plants, these physiological traits are not consistently correlated with N content (Rice et al., 2008; Wang et al., 2014). To date, no trait-based analyses have fully explored photosynthetic traits in bryophytes beyond basic light response and C assimilation (e.g., Rice et al., 2008; Wang et al., 2017). Examining characteristics of photosynthetic efficiency (e.g., using the chlorophyll fluorescence parameter F_v/F_m, the maximum quantum yield of photosystem II) and ecologically relevant C fixation traits (e.g., C-balance) may uncover examples of novel physiological traits. Further, aside from analyses on *Sphagnum*, no studies have examined within-clade functional trait diversity in bryophytes.

Syntrichia is a diverse clade consisting of approximately 80 terminal taxa worldwide (over 30 estimated in North America alone; Zander & Eckel, 1993; J. Brinda, personal communication), with representatives in ecosystems ranging from desert (e.g., Mojave Desert) to alpine (e.g., Rocky Mountains). Some *Syntrichia* are important constituents of soil biocrust communities that contribute to primary productivity, regulate ecosystem N availability, influence water retention, and stabilize soils in dryland ecosystems (Belnap, 2002; Belnap, 2006; Belnap & Lange, 2001; Bowker, Mau, Maestre, Escolar, & Castillo-Monroy, 2011; Maestre et al., 2011).

Several characteristics of *Syntrichia* have been identified as key functional traits that directly or indirectly influence ecosystem function. Carbon dioxide exchange, specifically the integrated net carbon balance following exposure to a rainfall event (hereafter, C-balance; Alpert & Oechel, 1985), has been linked to survival of moss communities in biocrusts (Coe, Belnap, & Sparks, 2012; Reed et al., 2012), C-cycling (Coe & Sparks, 2014), and N-cycling (Reed et al., 2012). Carbon balance may also be an important measure for quantifying desiccation tolerance (DT), the ability to completely lose water from tissues, then regain physiological functioning when hydration returns (Mishler & Oliver, 2009). Carbon balance may thus represent a unique physiological trait that acts as both a response and effect trait for mosses. Variability in C-balance in response to altered rainfall patterns has allowed for predictions about how biocrust mosses will respond to changing environmental conditions as well as the ecosystem level ramifications of changes in survival (Coe & Sparks, 2014); however, we currently possess this information only for a single species, *Syntrichia caninervis*. It is likely that variation in C-balance is present within *Syntrichia* and contributes to physiological performance, DT, and survival of individuals as well as ecology, biogeochemistry, biodiversity, and biogeography at larger scales. Further, how C-balance relates to other traits (such as morphological characteristics of leaves or cells or physiological traits like photosynthetic capacity) is unknown, but this information could represent an important resource for expanding bryophyte functional trait databases.

In this study, we focused on 14 genotypes representing 13 *Syntrichia* species common to North America and applied a functional trait-based approach to (a) examine how C-balance differs in the *Syntrichia* clade; (b) examine how 13 morphological and 10 physiological traits correlate with each other and with C-balance; (c) apply ordination techniques to examine clustering and variation among taxa in the 23 traits measured; and (d) develop models to predict C-balance based on suites of morphological and physiological traits. We hypothesized that C-balance exhibits variation among taxa and that this variation can be predicted based on suites of morphological and physiological traits. As C-balance can be time intensive and complicated to measure, we also aimed to develop a list of traits that can be measured to act as proxies for C-balance based on our modelling results.

2 | MATERIALS AND METHODS

2.1 | Moss culturing protocols

Mosses were cultured to remove their environmental history so that comparisons were being made of dehardened mosses (see Stark, 2017) with results reflecting the evolutionary rather than

environmental history of each species. *Syntrichia* samples (n = 3 per genotype) were grown in culture in lab facilities at St. Mary's College of Maryland, MD, USA from previously collected material. Information about each genotype including the location of herbarium vouchers can be found in Table S1. All samples were cultured in the lab asexually from pre-existing leaf or stem material and were grown for at least two months to ensure shoots had reached maturity prior to analyses. Moss cultures were grown in 35-mm-diameter Petri dishes containing autoclaved sand media and watered every other day with alternating applications of autoclaved reverse osmosis water and a 30% Hoagland's solution (Hoagland & Arnon, 1938). Samples were incubated in Percival I36LLVL growth chambers (Percival Scientific Inc., Perry, Iowa, USA) on a diurnal program; day settings were 20°C and 70% relative humidity with light at 100 μm m^{-2} s^{-1} and night settings were 8°C and 70% relative humidity.

2.2 | Determination of photosynthetic area for CO_2 exchange measurements

Photosynthetic area was measured by determining the average height of the moss and the area of the aerial view of the sample's photosynthetic tissue. Average moss height was measured using a narrow ruler at the centre of the dish and at 0.5 and 1 cm from the centre on perpendicular transects. The green photosynthetic tissue for each culture plate was photographed at approximately 200× magnification and used for measuring the aerial view if the sample's photosynthetic tissue with ImageJ2. The aerial view area and the average height of the moss were used to approximate the total photosynthetic area of the moss as the surface area of a cylinder. This method improves on previous work that capitalized on a relatively uniform and small depth of green photosynthetic tissue in *Syntrichia* cushions in order to measure photosynthesis on an area basis (Coe et al., 2012) by including height of cushions to enable comparisons across different genotypes of varying morphology.

2.3 | Desiccation of samples

Moss samples of sufficient photosynthetic area (2.5 cm^2 minimum, previously determined based on pilot CO_2 exchange data; n = 1–3 per genotype and 26 total), following approximately 6 months of growth, were dried using 33% Relative Humidity (RH) desiccators. The desiccators were made by adding 20 ml of water and approximately 12 g of $MgCl_2$ salt to 100-ml jars (Sigma-Aldrich, Milwaukee Wisconsin, USA). iButtons (Embedded Data Systems, Lawrenceburg Kentucky, USA) were used to ensure that the desiccators achieved 33% RH before moss samples were added. The samples were placed in the desiccators on top of 20-ml jars (Wheaton, Millville New Jersey, USA) filled with BB gun pellets out of contact with the $MgCl_2$ solution. Samples were checked once a day for dryness by noting degree of leaf curling, an indicator of dryness (Stark, 2017). All samples were dried slowly over approximately 5 days at 33% RH, and C-balance analyses were performed approximately 24 hr after plants were completely desiccated, based on presence of fully curled leaves, calibrated based on drying procedures above and those outlined in Stark (2017).

2.4 | Carbon balance data collection

Carbon balance measurements were performed with a Licor-6400XT (LICOR Biosciences, Lincoln Nebraska, USA) using an attached Licor bryophyte chamber. A 3D printer was used to construct an alternate bottom for the chamber that incorporated a port through which water could be added into the chamber. This was done so that CO_2 exchange measurements could begin prior to water being added to the closed system (i.e., when moss was still dry), ensuring accurate characterization of the often immediate initial release of CO_2 through respiration at the onset of rehydration (Coe et al., 2012; Mishler & Oliver, 2009). This plate was printed using Polylactic acid (PLA) plastic because it had a very low coefficient of diffusion to CO_2 (Jamshidian, Tehrany, Imran, Jacquot, & Desobry, 2010). Carbon dioxide diffusion through the printed plate was compared with that of the LICOR plate by recording the measured change in CO_2 within the chamber while it contained a Petri dish filled with sand and water. The 3D printed plate was determined to perform as well or better than the LICOR plate. During C-balance measurements, conditions in the bryophyte chamber were set to 400 ppm of CO_2 with a flow rate of 500 μmol s^{-1} and 1,000 μmol m^{-2} s^{-1} PAR using the included RGB light source. These conditions were selected based on previous studies using *S. caninervis* (Coe et al., 2012; Reed et al., 2012) and light response analyses conducted on a subset of the genotypes in this study.

To begin a C-balance measurement, a fully desiccated Petri dish of moss was enclosed in the sample chamber, and 1.8 ml of water was administered to the dish from above using the custom port. Based on a pilot study where samples of varying photosynthetic area were exposed to differing amounts of water, this amount was experimentally determined to be sufficient for hydrating all samples to full turgor, due to the humid environment of the small chamber. This enabled us to standardize the amount of water added to each sample, regardless of variations in sample size or texture. Carbon dioxide exchange measurements began prior to hydration and were recorded every 15 s throughout the ensuing wet–dry cycle using the Licor-6400XT autolog2 program.

Following CO_2 exchange data collection, C-balance curves were created by plotting photosynthesis (μmol CO_2 m^{-2} s^{-1}) over time (s). Total C-balance was determined by fitting these curves to a polynomial function and integrating the area under the curves using R version 3.4.4 (R Core Team, 2018). A C-balance curve for mosses typically consists of three phases (Coe et al., 2012; Mishler & Oliver, 2009): an initial loss of C from a respiratory burst upon rehydration (Phase A), a period of net C gain when the moss is hydrated and photosynthetically active (Phase B), and a small period of C loss as tissues approach desiccation again (Phase C). To examine these three phases independently, the net C fixed occurring in each phase of the curve was obtained by applying the polynomial fit as above and adjusting the limits of integration.

2.5 | Physiological traits

After each sample had been in the chamber undergoing measurements for approximately 1.5 hr, CO_2 exchange was manually checked every 10 min to determine when the sample achieved maximum photosynthesis. When no change (±0.1 μmol CO_2 m^{-2} s^{-1}) in photosynthesis was observed for 20 min, the bryophyte chamber's light source was turned off to allow the sample to dark adapt for 25 min. After this period, room lights were extinguished and the bryophyte chamber was opened underneath a black cloth. For each sample, we measured three physiological traits corresponding to photosynthetic capacity using chlorophyll fluorescence: maximum dark-adapted quantum yield of photosystem II (F_v/F_m), baseline variable chlorophyll fluorescence (F_o), and maximum chlorophyll fluorescence (F_m). To obtain F_v/F_m, F_o, and F_m measurements for the sample, the probe of a Walz Minipam chlorophyll fluorometer (Heinz Walz GmbH, Effeltrich, Germany) was held 1 cm away from the surface of the moss and a saturating pulse of light (approximately 2,500 μmol m^{-2} s^{-1}) was applied to the dark-adapted sample. The chamber was subsequently re-closed for the remainder of the C-balance curve.

Physiological trait data included in analyses were derived from CO_2 exchange as well as chlorophyll fluorescence measurements, and collectively included total C-balance, total C fixation in each of the A, B, and C phases of the C-balance curve, time to net CO_2 compensation point (Time Comp, when CO_2 exchange becomes positive; i.e., the transition from Phase A to Phase B), maximum rate of photosynthesis (A_{max}), time to maximum photosynthesis (Time A_{max}), total time of C-balance curve (Time Total), F_v/F_m, F_o, and F_m.

2.6 | Morphological traits

Morphological data collected for each sample included measurements of 13 different traits. Three shoots of each taxon were randomly selected from lab cultures and photographed at 10× for determination of shoot height (SH, mm). One leaf was removed from the midpoint of each shoot and photographed at 10× to evaluate lamina length (LL, mm), width (LW, mm), and area (LA, mm^2) and awn (hair point) presence, awn length (AL, mm), and length that was hyaline (i.e., containing colourless cells that are dead at maturity, AL (HY), mm). Leaves were subsequently photographed at 400× to measure cell lumen length (CLL, μm), width (CLW, μm), and area (CL L/W, $μm^2$) of midleaf cells. Finally, midleaf cross sections were photographed at 400× for the quantification of interior cell wall thickness (CWT, μm) and lamina thickness (LT, μm). Shoots and leaves were then dried for 48 hr at 60 C, and weighed to determine shoot mass (SM, mg). All shoot and leaf-level measurements were obtained using ImageJ (Rueden et al., 2017) from high resolution photographs of each *Syntrichia* sample using a digital camera attached to a Leica DME Compound Microscope or Leica MZ75 Dissecting Microscope (Leica, Inc., Heerbrugg, Switzerland).

2.7 | Data analysis

To examine overall variability in C-balance in *Syntrichia*, we compared mean (sample average) C-balance across all genotypes examined. The number of samples analysed per genotype ranged from 1 to 3, depending on the existence of sufficient photosynthetic area for accurate C exchange measurements (approximately 2.5 cm^2, based on pilot studies). To determine what relationships existed among the traits measured, including C-balance, we examined correlations between all traits using a correlation matrix. We then used nonmetric multidimensional scaling (NMDS; Kruskal, 1964) as a tool to summarize and visualize trait variation among genotypes and its relationship to C-balance. Prior to ordination, we rescaled all traits from 0 to 1 (relativized to maximum) to standardize their units and make them nondimensional. We then created a two-dimensional ordination of all morphological and physiological traits together based on a Euclidean distance matrix. Selection of dimensionality was based on the balance between complexity of presentation and stress; the final stress of the two-dimensional solution was satisfactory, and the decrease in stress from two to three dimensions was not sufficient to warrant inclusion of an extra axis. We rotated the resultant ordination to maximize the correlation of axis 1 with C-balance (McCune & Grace, 2002). Then, as an interpretive aid, we obtained Pearson correlation coefficients of each trait variable with the axes. We conducted our ordination using PC-ORD 6.08 (2011 MJM Software Design).

To test the hypothesis that variation in C-balance can be predicted based on suites of morphological and physiological traits, we performed two rounds of an iterative modelling process: one using all of the morphological traits and one using all of the physiological traits. It was not possible programmatically to produce a model including all traits collected because of the number of traits relative to number of genotypes. In each procedure, additive linear models were used to identify significant predictive variables for C-balance, and then backwards stepwise regression was used to establish candidate models (Table S2). Specifically, we used backwards stepwise regression to find the set of independent variables that best predicted C-balance by minimizing the sum squared of residuals (Cook & Weisberg, 1980). Best fit models using subsets of traits from the morphological, physiological, and combined datasets were identified based on *AIC* and subsequent interpretation of R^2 values.

3 | RESULTS

Syntrichia genotypes responded to the standardized desiccation and rehydration process with a wide range of C-balances, ranging from moderate C gains (e.g., *Syntrichi bartramii*, 8.542 mmol CO_2 m^{-2}) to large C losses (e.g., *Syntrichia chisosa*, −18.12 mmol CO_2 m^{-2}) and a mean value of −5.50 mmol CO_2 m^{-2} (Table 1). Among the 13 morphological traits measured, leaf area and cell lumen area displayed the most variability among genotypes. Leaf area ranged from 120 to 604 mm^2, and cell lumen area ranged from 41 to 461 $μm^2$. Leaf width was very consistent among genotypes, with a mean of 0.71 mm (0.23 SD). Awns were present in all but one genotype (*Syntrichia latifolia*), and when present, awn length ranged from 0.05 to 0.78 mm. Length of awn that was hyaline ranged from 0 (no hyaline cells present) to 0.59 mm. Among genotypes where awns were present,

TABLE 1 Mean values and standard error for 22 morphological and physiological functional traits for 14 North American *Syntrichia* genotypes (n = 3 for all morphological traits, n = 2 or more for physiological traits when *SE* are included)

	Bartramii	*Caninervis*	*Chisosa*	*Laevipila*	*Latifolia*	*Montana*	*Norvegica*
CLA	107.8 ± 10.1	122.7 ± 10.0	48.50 ± 3.8	130.1 ± 11.0	161.0 ± 7.50	83.00 ± 5.6	232.3 ± 21.4
CLL	8.541 ± 0.65	11.48 ± 0.95	7.016 ± 0.23	13.94 ± 0.50	14.29 ± 0.50	8.260 ± 0.47	14.46 ± 1.03
CLW	12.56 ± 0.75	12.59 ± 0.64	6.218 ± 0.32	11.14 ± 0.94	15.09 ± 0.51	11.03 ± 0.45	16.88 ± 0.89
Cl L/W	0.688 ± 0.08	0.924 ± 0.12	1.138 ± 0.10	1.273 ± 0.15	0.950 ± 0.05	0.753 ± 0.06	1.047 ± 0.12
CWT	1.468 ± 0.23	0.654 ± 0.10	1.407 ± 0.13	1.587 ± 0.35	1.355 ± 0.06	1.181 ± 0.18	0.961 ± 0.18
Lf L/W	3.297 ± 0.05	2.263 ± 0.25	3.286 ± 0.10	2.008 ± 0.06	2.456 ± 0.09	2.648 ± 0.11	2.004 ± 0.05
LW	0.679 ± 0.02	0.496 ± 0.07	0.569 ± 0.03	0.681 ± 0.00	1.115 ± 0.00	0.625 ± 0.03	1.006 ± 0.02
LL	2.237 ± 0.05	1.089 ± 0.04	1.876 ± 0.14	1.367 ± 0.04	2.738 ± 0.09	1.657 ± 0.13	1.994 ± 0.02
LA	0.003 ± 1.12e4	0.002 ± 0.84e4	0.002 ± 2.26e4	0.002 ± 1.47e4	0.002 ± 4.53e4	0.002 ± 3.82e4	0.005 ± 3.74e4
LT	22.43 ± 0.63	19.79 ± 1.40	21.45 ± 1.23	25.84 ± 1.35	22.43 ± 1.33	19.19 ± 0.99	30.35 ± 1.32
SH	3.559 ± 0.27	1.731 ± 0.27	1.422 ± 0.19	0.999 ± 0.08	3.875 ± 0.12	2.516 ± 0.03	5.007 ± 0.10
SM	0.418 ± 0.12	0.075 ± 0.01	0.417 ± 0.01	0.133 ± 0.03	0.639 ± 0.14	0.196 ± 0.01	0.387 ± 0.02
AL	0.321 ± 0.04	0.124 ± 0.02	0.066 ± 0.01	0.150 ± 0.02	n/a	0.183 ± 0.02	0.196 ± 0.03
AL (HY)	0.321 ± 0.04	0.046 ± 0.01	0.058 ± 0.02	0.108 ± 0.01	n/a	0.172 ± 0.02	0.105 ± 0.04
F_v/F_m	0.539 ± 0.09	0.523 ± 0.15	0.403 ± 0.03	0.457	0.549 ± 49.0e4	0.523 ± 0.15	0.539 ± 0.04
F_o	1,008 ± 110	589 ± 11	499 ± 85	461	802 ± 34	785 ± 200	306 ± 16
F_m	2,195 ± 45.0	1,300 ± 306	852.5 ± 167	850	1,780 ± 89.5	1,774 ± 780	670 ± 77
Time Comp	772.5 ± 683	4,791 ± 368	n/a	n/a	5,348 ± 4,910	2,378 ± 1,190	n/a
A_{max}	1.309 ± 0.14	0.300 ± 0.23	−0.155 ± 0.11	n/a	1.128 ± 0.01	1.012 ± 0.22	−0.012 ± 0.01
Time A_{max}	5,865 ± 4,530	7,568 ± 1,177	10,260 ± 1,575	n/a	9,165 ± 3,660	8,025 ± 30	5,108 ± 22.5
Time Total	21,435 ± 1,080	18,750 ± 750	18,640 ± 1,360	20,000	17,000 ± 3,000	15,750 ± 250	11,483 ± 263
CBal	8.543 ± 1.25	−4.655	−18.12 ± 4.73	−6.325	−4.463 ± 7.24	5.284 ± 2.66	−13.91 ± 10.1
	Obtusissima	*Pagorum*	*Papillosa*	*Princeps*	*Ruralis* CAN	*Ruralis* UT	*Sinensis*
CLA	280.2 ± 23.9	232.4 ± 18.0	349.4 ± 32.8	188.3 ± 14.2	106.0 ± 3.9	81.33 ± 8.2	173.8 ± 8.8
CLL	18.13 ± 0.81	14.30 ± 0.32	21.43 ± 2.36	13.33 ± 1.65	11.11 ± 0.78	10.03 ± 0.03	14.05 ± 1.79
CLW	17.25 ± 0.55	15.27 ± 0.35	19.67 ± 1.95	14.55 ± 1.38	10.97 ± 1.11	9.695 ± 0.80	14.38 ± 0.37
Cl L/W	1.055 ± 0.07	0.937 ± 0.02	1.093 ± 0.08	0.916 ± 0.06	1.043 ± 0.15	1.051 ± 0.09	0.984 ± 0.15
CWT	1.527 ± 0.18	1.489 ± 0.05	1.320 ± 0.04	1.319 ± 0.23	1.375 ± 0.35	1.020 ± 0.23	1.277 ± 0.09
Lf L/W	2.582 ± 0.06	1.741 ± 0.19	1.853 ± 0.26	2.098 ± 0.13	2.830 ± 0.22	2.723 ± 0.07	2.458 ± 0.13
LW	0.951 ± 0.06	1.065 ± 0.10	0.714 ± 0.04	0.609 ± 0.01	0.209 ± 0.02	0.545 ± 0.01	0.726 ± 0.07
LL	2.452 ± 0.13	1.816 ± 0.03	1.306 ± 0.12	1.276 ± 0.07	0.593 ± 0.08	1.482 ± 0.03	1.782 ± 0.18
LA	0.005 ± 1.77e4	0.004 ± 3.05e4	0.005 ± 3.62e4	0.004 ± 1.65e4	0.002 ± 0.53e4	0.002 ± 0.72e4	0.003 ± 1.27e4
LT	29.34 ± 1.30	35.97 ± 2.35	31.79 ± 3.06	28.98 ± 1.38	23.35 ± 0.57	20.94 ± 0.68	29.10 ± 1.91
SH	6.227 ± 0.38	1.486 ± 0.04	0.700 ± 0.17	2.331 ± 0.25	16.70 ± 0.65	3.628 ± 0.22	1.808 ± 0.09
SM	0.719 ± 0.14	0.400 ± 0.06	0.262 ± 0.05	0.229 ± 0.03	1.153 ± 0.19	0.563 ± 0.08	0.446 ± 0.11
AL	0.664 ± 0.06	0.568 ± 0.01	0.279 ± 0.07	0.148 ± 0.05	0.086 ± 0.01	0.547 ± 0.09	0.135 ± 0.02
AL (HY)	0.587 ± 0.03	0.326 ± 0.01	0.101 ± 0.01	0.091 ± 0.04	0	0.440 ± 0.08	0
F_v/F_m	0.519 ± 0.01	0.329	0.287	0.5	0.426 ± 0.13	0.553	0.613
F_o	992 ± 98	1,035	347	575	345 ± 12	461	552
F_m	2,064 ± 226	1,544	487	1,152	619.5 ± 118	1,032	1,429
Time Comp	n/a	n/a	n/a	555	n/a	1,440	4,545
A_{max}	n/a	−0.067	n/a	1.328	−0.292 ± 0.02	1.762	0.975

(Continues)

TABLE 1 (Continued)

	Obtusissima	*Pagorum*	*Papillosa*	*Princeps*	*Ruralis* CAN	*Ruralis* UT	*Sinensis*
Time A_{max}	n/a	15,615	n/a	4,035	11,678 ± 6,758	7,395	7,980
Time Total	20,183	23,000	24,990	16,000	23,108 ± 2,108	22,770	18,500
CBal	−6.804 ± 0.126	−13.20	−15.20	−9.747	−14.06 ± 3.84	−4.894 ± 3.23	−0.092

percent hyalinity ranged from (0% in *Syntrichia ruralis* CAN and *Syntrichia sinensis*) to 100 % (in *S. bartramii*) and had a median value of 61.5%. Among the 10 physiological traits measured, the integral of Phase C of the C-balance curve varied the most among genotypes, and ranged from 0 (i.e., not present) in six genotypes to −29.56 mmol CO_2 m^{-2} in *Syntrichia princeps*. Time to CO_2 compensation point also varied substantially among genotypes, with a mean value of 87 min (minimum = 1.5 min, maximum = 330 min). Three genotypes (*Syntrichia norvegica*, *S. chisosa*, and the *S. ruralis* genotype from Bow River, CAN) never reached CO_2 compensation throughout the curve, and CO_2 exchange remained negative the entire time.

Morphological traits at the shoot level (SM, SH) were positively correlated with leaf size (LL, LW; r = .50–.73) and some photosynthetic physiology traits (A_{max}, F_v/F_m; r = .54–0.76; Figure 1, Table S3). At the leaf level, leaf size (LA, LT) were positively correlated with several cell level traits (CLL, CLA; r = .49–.84), and relatively longer leaves (i.e., higher Lf L/W) were associated with higher C-balance (r = .83), F_o (r = .66), and F_m (r = .69). Awn traits (AL, AL (HY)) were positively correlated with A_{max} (r = .65–.68) and duration of C-balance curve (Time tot; r = .74–.81) but AL was negatively correlated with time to CO_2 compensation point (r = −.64). Physiological traits related to photosynthetic capacity (F_m, F_o) were positively correlated with C-balance (r = .73–.82) and leaf length (LL, Lf L/W; r = .66–.71) but negatively correlated with cell length:width (Cl L/W; r = −.82–(−.86)). Physiological traits associated with carbon balance curves (Time comp, Time A_{max}) were positively correlated with each other (r = .79) but negatively correlated with some leaf characteristics (AL, AL (HY), LA; r = −0.32–.71). On the other hand, the total time of the C-balance curve was positively correlated with awn characteristics (AL, AL (HY); r = .81 and r = .74, respectively).

Final stress of our two-dimensional NMDS analysis was 12.9, indicating a good representation of the data (McCune & Grace, 2002). After rotating, Axis 1 accounted for about one fifth of the variation (R^2 = .19), and Axis 2 accounted for about two thirds (R^2 = .67;

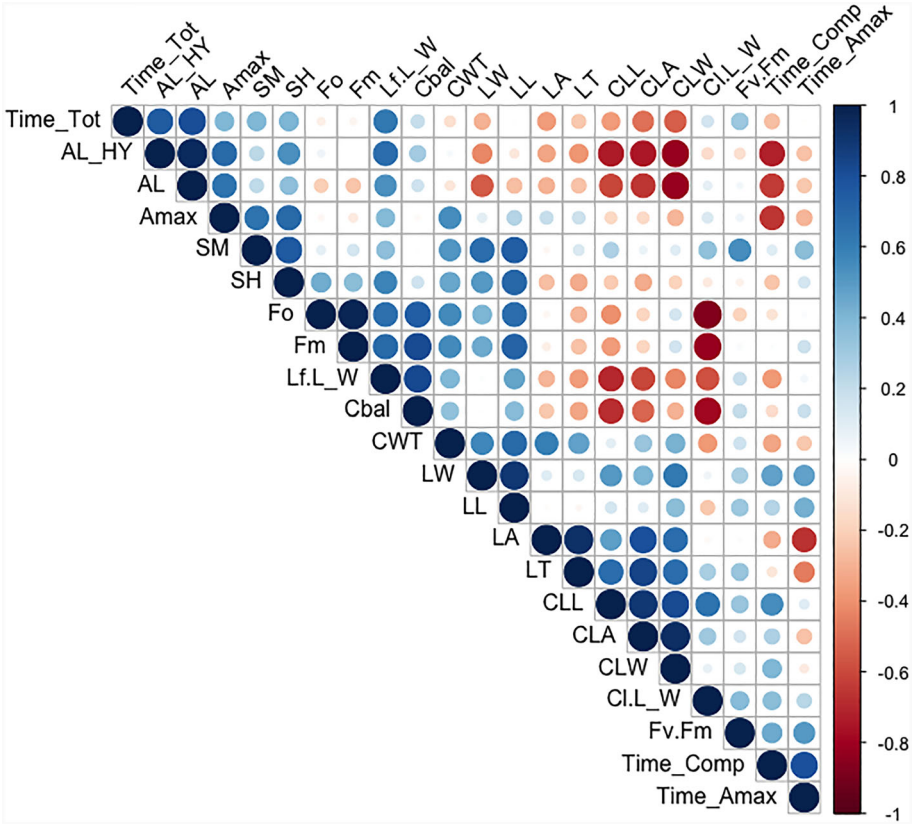

FIGURE 1 Correlogram displaying the degree of correlation between all traits measured, including morphological traits (AL (HY), AL, SM, SH, Lf L/W, CWT, LW, LL, LA, LT, CLL, CLA, Cl L/W), physiological traits (Time Tot, A_{max}, F_o, F_m, F_v/F_m, Time Comp, Time A_{max}), and carbon balance (CBal). Blue circles of strongest hue represent the strongest positive correlations, and red circles of strongest hue represent the strongest negative correlations [Colour figure can be viewed at wileyonlinelibrary.com]

Figure 2). C-balance was well-correlated to Axis 2 (r = .63), and independent of axis two (r = −.09), thus individual traits that correlate with Axis 1 can be interpreted to be correlated to C-balance. Three traits in particular stood out as being strongly positively correlated with Axis 1: F_m (r = .86), F_o (r = .75), and LL (r = .70). Several additional traits were more moderately correlated, some positively and some negatively (Table S3). Axis 2, which had little to do with C-balance, but was the dominant axis separating species in trait space, was most strongly correlated, negatively, with awn traits (AL: r = −.87, AH: r = −.82), and moderately correlated with several other morphological and physiological traits (Figure 2, Table S3).

The iterative backwards stepwise regression process produced eight candidate models for explaining C-balance through morphological and physiological traits (Table S2). Based on parsimony and AIC (which includes information on the number of parameters estimated), one morphological model and one physiological model were identified as the best models of C-balance (Table 2). The morphological model included leaf area, awn length, leaf width, leaf length, leaf length to width ratio, and cell lumen length to width ratio (R^2 = .80, F = 4.54, P = .034, AIC = 22.34). The physiological model included time to compensation point, total time, and the interactions between F_v/F_m and F_m, F_v/F_m and the integral of Phase A, and F_v/F_m and the integral and Phase B to explain total C-balance (R^2 = .86, F = 4.05, P = .099, AIC = 6.614).

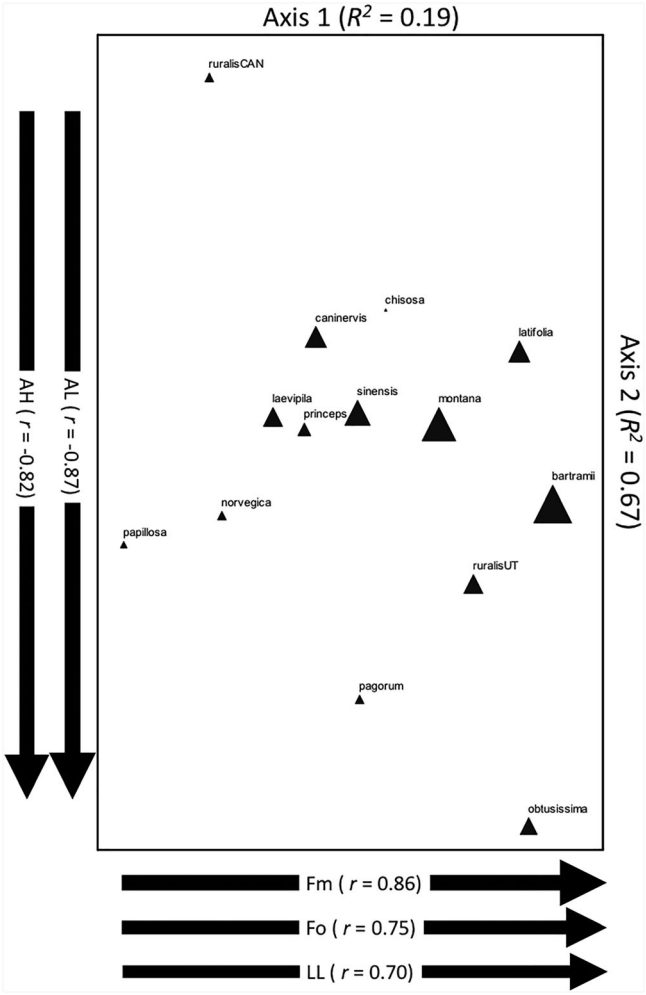

FIGURE 2 Nonmetric multidimensional scaling ordinations of *Syntrichia* genotypes, illustrating selected correlations between genotypes and particular traits. Symbols are sized according to mean C-balance for each genotype, where largest symbols show highest C-balance. For scale, the largest triangle represents a C-balance of 8.542 mmol CO_2 m^{-2}, and the smallest triangle represents a C-balance of −18.12 mmol CO_2 m^{-2}. Variables correlated with Axis 1 were maximum variable chlorophyll fluorescence under saturating light (F_m), baseline chlorophyll fluorescence (F_o), and leaf length (LL). Variables correlated with Axis 2 were awn length (AL) and degree of awn hyalinity (AL (HY))

4 | DISCUSSION

The rapid development of trait-based approaches has had a resounding influence on plant ecology and has helped us understand controls on ecosystem function (Gross et al., 2017) and the coexistence of species (Kraft, Godoy, & Levine, 2015). However, this impact has largely been confined to vascular plant communities, because functional traits of other plant and primary producer groups, like bryophytes, remain underdocumented (Cornellisen et al. 2007), despite that they are dominant in a substantial proportion of Earth's ecosystems. We cannot fully connect plant form and function with ecosystem processes until this knowledge gap is filled.

4.1 | Variation in the functional trait C-balance in *Syntrichia*

Among the 14 genotypes examined, only two (*S. bartramii* and *Syntrichia montana*) exhibited positive C-balance over the course of simulated precipitation events, whereas the remaining 12 exhibited negative C-balances (lost C) ranging from close to zero (*S. sinensis*) to strongly negative (*S. chisosa*). The presence of this broad range from C gains to C losses was expected. For one, the genotypes

TABLE 2 Best fit morphological and physiological additive linear models for C-balance based on AIC

Morphological model		Physiological model	
Intercept	46.57	Intercept	−9.739
Leaf area	−0.477	Time to compensation point	0.578
Leaf width	−3.579	Total C-balance curve time	−1.915
Leaf length	3.674	F_v/F_m * F_m	−0.623
Leaf length:width	−3.879	F_v/F_m * F_0	0.769
Cell lumen length: width	−1.663	F_v/F_m * Integral of Phase A	0.379
Awn length	0.126	F_v/F_m * Integral of Phase B	0.086
F	4.54	F	4.05
R^2	.795	R^2	.859
P	.034	P	.098

Note. Coefficients reported are for traits identified in each of two best fit models using morphological and physiological data. For information on abbreviations and units, see Table S4.

(representing 13 different species) possess diverse morphological and physiological adaptations to a range of environments, and the observed range of C-balances may be related to how genotypes with different shoot and canopy architecture patterns responded physiologically to the standardized rainfall event size. The simulated precipitation amount for samples was equivalent to 1.8 mm in the field, which is very close to the hypothesized threshold for C gains in *S. caninervis* of approximately 2 mm (Barker, Stark, Zimpfer, Mcletchie, & Smith, 2005; Coe et al., 2012; Stark, 2005), but many species of *Syntrichia* occur in habitats with higher rainfall than *S. caninervis* and may be adapted to larger precipitation amounts. Although it was determined that the simulated precipitation event size was sufficient to hydrate all samples to full turgor (see Section 2), it is also possible that the visual distinction between full turgor and prehydration phenotypes that appear similar to full turgor was unclear. This experiment provided for a standardized comparison among genotypes for one level of precipitation. In the future, studies using a range of precipitation levels or a standardized amount of water per estimated total canopy leaf area will help to characterize the relationship between physiology and environment more clearly.

4.2 | Mechanistic relationships between C-balance, morphological, and physiological traits

We found that intrinsic differences in C-balance are correlated with sets of traits that might influence C uptake; we identified several suites of traits that were consistently associated with higher or lower C-balances. The highest C-balances were achieved in genotypes with narrow, long leaves that have long hyaline awns, and small cells with thick cell walls; lowest C-balances occurred in genotypes with rounder, awnless leaves with large cells (Figure 3). Leaf length and awn presence were also associated with higher maximum rates of photosynthesis (A_{max}) and higher baseline and maximum chlorophyll fluorescence (F_o and F_m) during the simulated rainfall event. The two-dimensional NMDS analysis further supported these morphological and physiological correlates of C-balance, where leaf length and fluorescence parameters aligned with the axis with the strongest correlation with C-balance ($r > .70$).

These suites of traits at the leaf and cell level may reflect adaptations for maximizing C uptake while reducing rates of water loss. Specifically, possession of small, narrow leaves may allow for a high surface area for CO_2 uptake via diffusion while also acting as a water conserving adaptation that enables plants to reduce transpiration (Yates, Verboom, Rebelo, & Cramer, 2010). Cell shape has been shown to correlate with hydraulic conductivity in vascular plants (Brodribb, Field, & Jordan, 2007), and our data suggest that it may also play a role in C exchange in bryophytes. Small cell volume, which was associated with higher C-balance in *Syntrichia*, has been observed in several other DT lichens and mosses and may allow for efficient utilization of small amounts of water (Dilks & Proctor, 1979). Thick cell walls, which we show are positively correlated with C-balance and maximum photosynthetic rate, likely afford plants additional water storage in apoplast space over the course of a hydration event (Honneger 1991).

The role of awns in bryophyte water relations has received much research attention; awns can decrease boundary layer conductance in bryophytes (Proctor, 1980); collect water from humid atmospheres, fog, and water droplets (Pan et al., 2016); and can influence leaf spreading during rehydration (Wu et al., 2014). Here, we show that awn length and degree of hyalinity also relate to A_{max} and C-balance and that genotypes with longer awns appear to reach the CO_2 compensation point (achieving net positive C uptake) earlier. We also show that awn length is positively correlated with the total duration of the C-balance curve (i.e., the period of hydration from the simulated rain event). It is possible that awns allow for efficient water uptake and subsequent reinstatement of metabolic activities and also may act to retard rates of water loss as tissues dry. Such inhibition of water loss during a rainfall event has been observed in other acrocarpous mosses with similar growth forms to *Syntrichia* (Proctor, 1980). The presence of hyaline cells in leaves of *Sphagnum* has long been observed as a strategy for water storage (Hayward & Clymo, 1982). However, it remains to be seen whether hyaline cells in awns may

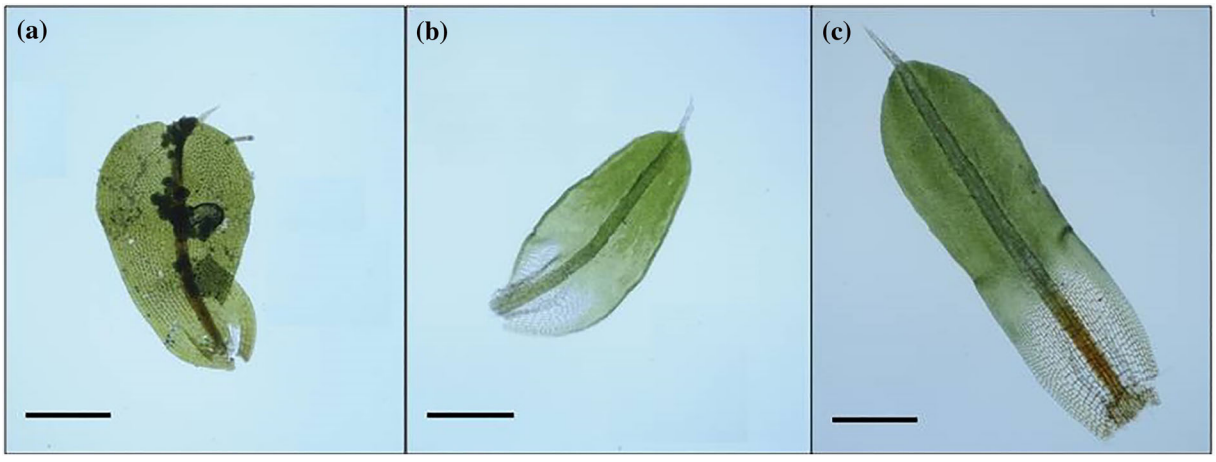

FIGURE 3 Examples of leaves from *Syntrichia* taxa exhibiting low (*Syntrichia papillosa*; a), intermediate (*Syntrichia caninervis*; b), and high (*Syntrichia bartramii*; c), carbon balances in this study. Scale bars: 0.5 mm [Colour figure can be viewed at wileyonlinelibrary.com]

function similarly, particularly those at the base of the awn, or if the role of awns in water conservation in *Syntrichia* and mosses of related growth forms is restricted to manipulations of the boundary layer.

4.3 | Relationships among *Syntrichia* genotypes in two-dimensional trait space

We expected that *Syntrichia* genotypes would exhibit distinct clustering in two-dimensional space based on our NMDS ordination and C-balance characteristics. Mosses exhibiting DT have been described as falling along a spectrum ranging from those that are constitutively tolerant, with mechanisms constantly present to protect against damage from desiccation, and those that are inducible, responding to signals from the environment to initiate repair–recovery mechanisms (Stark & Brinda, 2015; reviewed in Stark, 2017), and we expected that our ordination would place *Syntrichia* taxa along this spectrum. Other than the tight pairing of *Syntrichia laevipila*, *S. princeps*, and *S. sinensis* in the centre of the ordination, we did not observe distinct clustering of genotypes, but several patterns emerged related to C-balance and key traits. *S. bartramii*, *S. montana*, *S. ruralis* (UT), and *S. latifolia* exhibited the highest C-balances and were located towards the upper end of Axis 1. *S. caninervis* was positioned in the centre of the ordination, in close proximity to the *laevipila–princeps–sinensis* group. Surprisingly, the *S. ruralis* genotype from Bow River (CAN) was positioned in the upper left of the ordination, very far from *S. ruralis* (UT). This was due to a combination of trait differences; compared with *S. ruralis* (UT), *S. ruralis* (CAN) has smaller leaves, shorter awns, lower F_o and F_m, and a lower C-balance. The observed large distance in NMDS space and associated differences in C-balance between these two genotypes of *S. ruralis* may be related to the diverse range of global environments occupied by this species and associated genetic differences across its range. *S. ruralis* as currently understood is a cosmopolitan species occurring along wide elevational gradients on all continents except Antarctica and Australia (Table S1; Mishler, 2007), can occupy substrates from dry to moist soil as well as rock, and has been shown to exhibit variability in genomic structure even within a relatively small geographical region (i.e., The Colorado Plateau, USA; Massatti, Doherty, & Wood, 2018). It may well represent a complex of distinct clades, which our group is pursuing in separate taxonomic studies.

Based on these collective results across *Syntrichia* genotypes, it appears that photosynthetic recovery from a relatively slow dry event is best achieved in certain morphotypes (small, long leaves with small, thick walled cells, and hyaline awns) and that these characteristics can lead to higher photosynthetic capacity during the hydration period. As all samples were exposed to a slow drying event prior to C-balance measurements (conditions that, in nature, could lead to expression of DT phenotypes in inducible genotypes), it is possible that the suites of traits that led to higher C-balances here are generally reflective of a stronger inducibility of DT. However, DT represents a large set of processes operating before, during, and following a period of desiccation, and these patterns do not allow us to directly compare taxa in terms of overall DT. Importantly, they do allow for characterization of trait-based variability that, when combined with evidence from physiological experiments, may allow us to infer groupings of taxa that exhibit similar mechanisms for DT. Specifically, future work involving additional ecological (e.g., patterns of water availability in the environments occupied by different taxa), physiological (i.e., minimum rate of drying), and molecular (transcriptomic profiles at different stages of recovery) data will help create a holistic understanding of DT in this clade.

4.4 | Effectively predicting C-balance from easily measured traits

Although C-balance is an important functional trait in bryophytes, and especially DT bryophytes, obtaining a single C-balance value for a sample requires a lengthy multiday procedure using non-standard ecophysiology equipment. For this reason, our morphological and physiological models for C-balance provide relatively easier measurements that can act as proxies for C-balance. Our best fit morphological model for C-balance included many of the predictors of C-balance also observed in our trait correlation and ordination analyses (leaf area and length, cell size, and awn length), whereas our best fit physiological model included some additional traits related to but not identified in the correlation and ordination analyses. Specifically, it appears that completing an entire C-balance curve, while yielding a wealth of detailed information about physiological recovery from desiccation events, may not be required if just the single C-balance value is desired. Our physiological model suggests that shortened experiments that gather information like time to CO_2 compensation point, the integral of Phase A, or F_v/F_m at maximum photosynthesis during Phase B may be sufficient at estimating C-balance. Experiments completing a partial C-balance curve that ceases after 1–2 hr with a measurement of F_v/F_m, or potentially measurement of F_v/F_m following a simple standardized laboratory hydration under light-saturated conditions, may yield useful photosynthetic capacity data indicative of C-balance. Finally, our analyses show that our predictive models for C-balance are better determined by measurement of traits versus genotype (as exemplified by C-balance and NMDS distance in the two genotypes of *S. ruralis*), thus can be applied to intraspecific as well as interspecific variation in this clade.

4.5 | Future directions for bridging the form-function gap and trait-based approaches in bryophytes

Here, we show that *Syntrichia*, a diverse clade of dryland mosses, exhibits substantial variation in C-balance, a key functional trait that is related to physiological performance, survival, and, due to the role of *Syntrichia* in biocrust communities, ecosystem function. Further, we show that suites of morphological and physiological traits correlate with C-balance and each other and present two models to best predict C-balance.

The variability in C-balance and its associated traits in *Syntrichia* shown here represents the beginning of a framework for mapping and analysing physiological and anatomical functional traits in dryland bryophytes, many of which are key components of biocrust communities. As variation in C-balance has consequences at the organism as well as ecosystem scale (Coe et al., 2012; Coe & Sparks, 2014; Reed et al., 2012), development of such databases and modelling efforts can aid in predictions for the influences of environmental change on ecosystems where nonvascular plants play large ecological roles (i.e., drylands, boreal forests, peatlands). Given the variability of predictions for dryland ecosystems under global change (IPCC, 2014), the variability in C-balance observed here may also assist in predictions for biodiversity and ecosystem function in these systems. Moreover, many of the traits that we show are significant predictors of C-balance are relatively simple to measure, which facilitates their inclusion in functional trait databases for bryophytes. Future studies are planned by our group to place these comparisons into a phylogenetic and environmental context, to pursue further tests of adaptive hypotheses about plant traits.

ACKNOWLEDGEMENTS

This research was supported by the National Science Foundation Dimensions of Biodiversity Program Awards 1638955 (to K. K. C.), 1638966 (to M. A. B.), 1638956 (to B. D. M.), and 1638943 (to L. R. S.). The authors also wish to thank Elaine Szymkowiak, Tom Brewer, Katrina Golladay, Dylan Powell, and Kelly Healy for assistance and support with moss culturing at St. Mary's College of Maryland. M. L. S. and R. B. thank the National Science Foundation Graduate Research Fellowship and the UM Drollinger-Dial award for support. The authors also thank 3D MOSS collaborators John Brinda, Theresa Clark, Mel Oliver, and Kirsten Fisher for valuable input on this study.

ORCID

Kirsten K. Coe https://orcid.org/0000-0002-1560-8022
Joshua Greenwood https://orcid.org/0000-0002-8334-5308

REFERENCES

Alpert, P., & Oechel, W. C. (1985). Carbon balance limits the microdistribution of *Grimmia laevigata*, a desiccation-tolerant plant. *Ecology*, *66*, 660–669.

Anderegg, W. R. (2015). Spatial and temporal variation in plant hydraulic traits and their relevance for climate change impacts on vegetation. *New Phytologist*, *205*, 1008–1014.

Barker, D. H., Stark, L. R., Zimpfer, J. F., Mcletchie, N. D., & Smith, S. D. (2005). Evidence of drought-induced stress on biotic crust moss in the Mojave Desert. *Plant, Cell and Environment*, *28*, 939–947.

Belnap, J. (2002). Nitrogen fixation in biological soil crusts from southeast Utah, USA. *Biology and Fertility of Soils*, *35*, 128–135. https://doi.org/10.1007/s00374-002-0452-x

Belnap, J. (2006). The potential roles of biological soil crusts in dryland hydrologic cycles. *Hydrological Processes*, *20*, 3159–3178. https://doi.org/10.1002/hyp.6325

Belnap, J., & Lange, O. L. (2001). Structure and functioning of biological soil crusts: A synthesis. In J. Belnap, & O. L. Lange (Eds.), *Biological soil crusts: Structure, function, and management* (pp. 471–479). Berlin, Heidelberg: Springer.

Bowker, M. A., Mau, R. L., Maestre, F. T., Escolar, C., & Castillo-Monroy, A. P. (2011). Functional profiles reveal unique ecological roles of various biological soil crust organisms. *Functional Ecology*, *25*, 787–795.

Brodribb, T. J., Field, S., & Jordan, G. J. (2007). Leaf maximum photosynthetic rate and venation are linked by hydraulics. *Plant Physiology*, *144*, 1890–1898.

Cadotte, M. W., Cavender-Bares, J., Tilman, D., & Oakley, T. H. (2009). Using phylogenetic, functional and trait diversity to understand patterns of plant community productivity. *PloS one*, *4*, e5695.

Coe, K. K., Belnap, J., & Sparks, J. P. (2012). Precipitation-driven carbon balance controls survivorship of desert biocrust mosses. *Ecology*, *93*, 1626–1636.

Coe, K. K., & Sparks, J. P. (2014). Physiology-based prognostic modeling of the influence of changes in precipitation on a keystone dryland plant species. *Oecologia*, *176*, 933–942.

Cook, R. D., & Weisberg, S. (1980). *Influence measures for robust regression*. Minneapolis, Minnesota: University of Minnesota.

Cornelissen, J. H., Lang, S. I., Soudzilovskaia, N. A., & During, H. J. (2007). Comparative cryptogam ecology: A review of bryophyte and lichen traits that drive biogeochemistry. *Annals of Botany*, *99*, 987–1001.

Cornelissen, J. H. C., Lavorel, S., Garnier, E., Diaz, S., Buchmann, N., Gurvich, D. E., & Pausas, J. G. (2003). A handbook of protocols for standardised and easy measurement of plant functional traits worldwide. *Australian Journal of Botany*, *51*, 335–380. https://doi.org/10.1071/BT02124

Cornwell, W. K., Cornelissen, J. H., Amatangelo, K., Dorrepaal, E., Eviner, V. T., Godoy, O., & Quested, H. M. (2008). Plant species traits are the predominant control on litter decomposition rates within biomes worldwide. *Ecology Letters*, *11*, 1065–1071.

Craine, J. M., Tilman, D., Wedin, D., Reich, P., Tjoelker, M., & Knops, J. (2002). Functional traits, productivity and effects on nitrogen cycling of 33 grassland species. *Functional Ecology*, *16*, 563–574.

Deane-Coe, K. K., & Stanton, D. (2017). Functional ecology of cryptogams: Scaling from bryophyte, lichen, and soil crust traits to ecosystem processes. *New Phytologist*, *213*, 993–995.

Díaz, S., Kattge, J., Cornelissen, J. H., Wright, I. J., Lavorel, S., Dray, S., & Garnier, E. (2016). The global spectrum of plant form and function. *Nature*, *529*, 7585.

Dilks, T. J. K., & Proctor, M. C. F. (1979). Photosynthesis, respiration and water content in bryophytes. *New Phytologist*, *82*, 97–114.

Gitay, H., & Noble, I. R. (1997). What are functional types and how should we seek them? In T. M. Smith, H. H. Shugart, & F. I. Woodward (Eds.), *Plant functional types: Their relevance to ecosystem properties and global change* (pp. 3–19). Cambridge: United Kingdom.

Gross, N., le Bagousse-Pinguet, Y., Liancourt, P., Berdugo, M., Gotelli, N. J., & Maestre, F. T. (2017). Functional trait diversity maximizes ecosystem multifunctionality. *Nature Ecology and Evolution*, *1*, 0132.

Hayward, P. M., & Clymo, R. S. (1982). Profiles of water content and pore size in Sphagnum and peat, and their relation to peat bog ecology. *Proceedings of the Royal Society of London Series B Biological Sciences*, *215*, 299–325.

Hoagland, D. R., & Arnon, D. I. (1938). *The water-culture method for growing plants without soil* (Vol. 347) (pp. 1–39). Davis, California: Circular. California Agricultural Experiment Station.

IPCC (2014). In R. K. Pachauri, et al. (Eds.), *Climate Change 2014: Synthesis Report Contribution of Working Groups I, II and III to the Fifth Assessment*

Report of the Intergovernmental Panel on Climate Change. In Core Writing Team, R.K. Pachauri & L.A. Meyer (Eds.) (p. 151). Geneva, Switzerland: IPCC.

Jamshidian, M., Tehrany, E. A., Imran, M., Jacquot, M., & Desobry, S. (2010). Poly-Lactic Acid: production, applications, nanocomposites, and release studies. *Comprehensive reviews in food science and food safety*, *9*(5), 552–571.

Kraft, N. J. B., Godoy, O., & Levine, J. M. (2015). Plant functional traits and the multidimensional nature of species coexistence. *Proceedings of the National Academy of Sciences*, *112*, 797–802.

Kraichak, E. (2012). Asexual propagules as an adaptive trait for epiphylly in tropical leafy liverworts Lejeuneaceae. *American Journal of Botany*, *99*, 1436–1444.

Kruskal, J. B. (1964). Nonmetric multidimensional scaling: A numerical method. *Psychometrika*, *29*, 115–129. https://doi.org/10.1007/BF02289694

Laing, C. G., Granath, G., Belyea, L. R., Allton, K. E., & Rydin, H. (2014). Tradeoffs and scaling of functional traits in *Sphagnum* as drivers of carbon cycling in peatlands. *Oikos*, *123*, 817–828.

Lavorel, S., & Garnier, É. (2002). Predicting changes in community composition and ecosystem functioning from plant traits: Revisiting the Holy Grail. *Functional ecology*, *16*, 545–556.

Lavorel, S., McIntyre, S., Landsberg, J., & Forbes, T. D. A. (1997). Plant functional classifications: From general groups to specific groups based on response to disturbance. *Trends in Ecology Evolution*, *12*, 474–478.

Lindo, Z., & Gonzalez, A. (2010). The bryosphere: An integral and influential component of the Earth's biosphere. *Ecosystems*, *13*, 612–627.

Maestre, F. T., Bowker, M. A., Cantón, Y., Castillo-Monroy, A. P., Cortina, J., Escolar, C., & Martínez, I. (2011). Ecology and functional roles of biological soil crusts in semi-arid ecosystems of Spain. *Journal of Arid Environments*, *75*, 1282–1291.

Mallen-Cooper, M., & Eldridge, D. J. (2016). Laboratory-based techniques for assessing the functional traits of biocrusts. *Plant and Soil*, *406*, 131–143.

Marschall, M., & Proctor, M. C. (2004). Are bryophytes shade plants? Photosynthetic light responses and proportions of chlorophyll a, chlorophyll b and total carotenoids. *Annals of Botany*, *94*, 593–603.

Massatti, R., Doherty, K. D., & Wood, T. E. (2018). Resolving neutral and deterministic contributions to genomic structure in Syntrichia ruralis (Bryophyta, Pottiaceae) informs propagule sourcing for dryland restoration. *Conservation genetics*, *19*(1), 85–97. https://doi.org/10.1007/s10592-017-1026-7

Matheny, A. M., Mirfenderesgi, G., & Bohrer, G. (2017). Trait-based representation of hydrological functional properties of plants in weather and ecosystem models. *Plant diversity*, *39*, 1–12.

McCune, B., & Grace, J. B. (2002). *Analysis of ecological communities*. Gleneden Beach, Oregon: MjM Software Design.

Mishler, B. D. (2007). Syntrichia. In Flora of North America Editorial Committee (Ed.), *1993 + Flora of North America North of Mexico, 20 + vols* (Vol. 27) (pp. 618–628). New York and Oxford: Flora of North America Association.

Mishler, B. D., & Oliver, M. J. (2009). Putting Physcomitrella patens on the tree of life: The evolution and ecology of mosses. In C. D. Knight, P. Perroud, & D. J. Cove (Eds.), *Annual Plant Reviews Volume 36: The Moss Physcomitrella patens* (pp. 1–15). West Sussex, UK: Wiley-Blackwell.

Pan, Z., Pitt, W. G., Zhang, Y., Wu, N., Tao, Y., & Truscott, T. T. (2016). The upside-down water collection system of *Syntrichia caninervis*. *Nature Plants*, *2*, 16076.

Proctor, M. C. F. (1980). Diffusion resistance of bryophytes. In J. Grace, E. D. Ford, & P. G. Jarvis (Eds.), *Plants and Their Atmospheric Environment* (pp. 219–229). Oxdford: Blackwell's Scientific Publication.

R Core Team (2018) R: A Language and Environment for Statistical Computing. R Foundation for Statistical Computing, Vienna. https://www.R-project.org

Reed, S. C., Coe, K. K., Sparks, J. P., Housman, D. C., Zelikova, T. J., & Belnap, J. (2012). Changes to dryland rainfall result in rapid moss mortality and altered soil fertility. *Nature Climate Change*, *2*, 752.

Rice, S. K., Aclander, L., & Hanson, D. T. (2008). Do bryophyte shoot systems function like vascular plant leaves or canopies? Functional trait relationships in Sphagnum mosses Sphagnaceae. *American Journal of Botany*, *95*, 1366–1374.

Rueden, C. T., Schindelin, J., Hiner, M. C., DeZonia, B. E., Walter, A. E., Arena, E. T., & Eliceiri, K. W. (2017). ImageJ2: ImageJ for the next generation of scientific image data. *BMC Bioinformatics*, *18*, 529.

Shaw, A. J., & Gaughan, J. F. (1993). Control of sex-ratios in haploid populations of the moss, *Ceratodon purpureus*. *American Journal of Botany*, *80*, 584–591.

Slate, M. L., Rosenstiel, T. N., & Eppley, S. M. (2017). Sex-specific morphological and physiological differences in the moss *Ceratodon purpureus* (Dicranales). *Annals of Botany*, *120*, 845–854. https://doi.org/10.1093/aob/mcx071

Stark, L. R. (2005). Phenology of patch hydration, patch temperature and sexual reproductive output over a four-year period in the desert moss *Crossidium crassinerve*. *Journal of Bryology*, *27*, 231–240.

Stark, L. R. (2017). Ecology of desiccation tolerance in bryophytes: A conceptual framework and methodology. *The Bryologist*, *120*, 130–165.

Stark, L. R., & Brinda, J. C. (2015). Developing sporophytes transition from an inducible to a constitutive ecological strategy of desiccation tolerance in the moss *Aloina ambigua*: Effects of desiccation on fitness. *Annals of Botany*, *115*, 593–603.

Street, L. E., Subke, J. A., Sommerkorn, M., Sloan, V., Ducrotoy, H., Phoenix, G. K., & Williams, M. (2013). The role of mosses in carbon uptake and partitioning in arctic vegetation. *New Phytologist*, *199*, 163–175.

Suding, K. N., Lavorel, S., Chapin, F. S., Cornelissen, J. H., Diaz, S., Garnier, E., & Navas, M. L. (2008). Scaling environmental change through the community-level: A trait-based response-and-effect framework for plants. *Global Change Biology*, *14*, 1125–1140.

Turetsky, M. R. (2003). The role of bryophytes in carbon and nitrogen cycling. *The Bryologist*, *106*, 395–409. https://doi.org/10.1639/05

Turetsky, M. R., Bond-Lamberty, B., Euskirchen, E., Talbot, J., Frolking, S., McGuire, A. D., & Tuittila, E. S. (2012). The resilience and functional role of moss in boreal and arctic ecosystems. *New Phytologist*, *196*, 49–67.

Waite, M., & Sack, L. (2010). How does moss photosynthesis relate to leaf and canopy structure? Trait relationships for 10 Hawaiian species of contrasting light habitats. *New Phytologist*, *185*, 156–172.

Wang, Z., Bader, M. Y., Liu, X., Zhu, Z., & Bao, W. (2017). Comparisons of photosynthesis-related traits of 27 abundant or subordinate bryophyte species in a subalpine old-growth fir forest. *Ecology and evolution*, *7*, 7454–7461.

Wang, Z., Bao, W., Feng, D., & Lin, H. (2014). Functional trait scaling relationships across 13 temperate mosses growing in wintertime. *Ecological Research*, *29*, 629–639.

Weiner, J., Campbell, L. G., Pino, J., & Echarte, L. (2009). The allometry of reproduction within plant populations. *Journal of Ecology*, *97*, 1220–1233.

Wright, I. J., Reich, P. B., Westoby, M., Ackerly, D. D., Baruch, Z., Bongers, F., et al. (2004). The worldwide leaf economics spectrum. *Nature*, *428*, 821–827.

Wu, N., Zhang, Y. M., Downing, A., Aanderud, Z. T., Tao, Y., & Williams, S. (2014). Rapid adjustment of leaf angle explains how the desert moss, *Syntrichia caninervis*, copes with multiple resource limitations during rehydration. *Functional Plant Biology*, *41*, 168–177.

Yates, M. J., Verboom, A., Rebelo, A. G., & Cramer, M. D. (2010). Ecophysiological significance of leaf size variation in Proteaceae from the Cape Floristic Region. *Functional Ecology*, *24*, 485–492.

Zander, R. H., & Eckel, P. M. (1993). *Genera of the Pottiaceae: mosses of harsh environments*. Buffalo, New York: Buffalo Society of Natural Sciences.

SUPPORTING INFORMATION

Additional supporting information may be found online in the Supporting Information section at the end of the article.

Table S1. Collector, locality, and voucher specimen data from which single genotype cultures were derived for use in the present study.

Table S2: Model selection and comparison of models using physiological (A) and morphological (B) variables to predict carbon balance.

Table S3: Correlation table displaying correlation coefficients for among all morphological and physiological variables measured.

Table S4: Abbreviations used in manuscript

How to cite this article: Coe KK, Howard NB, Slate ML, et al. Morphological and physiological traits in relation to carbon balance in a diverse clade of dryland mosses. *Plant Cell Environ*. 2019;1–12. https://doi.org/10.1111/pce.13613